Elliptical beams in CMB temperature and polarization anisotropy experiments: An analytic approach

P. Fosalba,* O. Doré,† and F. R. Bouchet‡
Institut d'Astrophysique de Paris, 98bis, boulevard Arago, F-75014 Paris, France
(Received 20 July 2001; published 15 February 2002)

We present an analytic approach to the estimation of beam asymmetry effects in cosmic microwave background (CMB) temperature and linear polarization anisotropy experiments. We derive via perturbative expansions simple and accurate results for the case of an elliptical Gaussian window. Our results are applied to investigate the effect of beam ellipticity in the estimation of full-sky polarization correlation functions and the covariance matrix of power spectra. The relevance of this effect is also discussed by forecasting errors including beam asymmetry for current and future cosmic microwave background (CMB) experiments.

DOI: 10.1103/PhysRevD.65.063003 PACS number(s): 98.70.Vc

I. INTRODUCTION

As high-resolution cosmic microwave background (CMB) experiments explore smaller fluctuations in the temperature anisotropy with high sensitivity, a better understanding of systematic effects is required to make more accurate measurements. These systematics have a direct impact on the ability we have to improve the process of CMB data analysis at the level of map making, power spectrum estimation and ultimately in constraining cosmological parameters.

A common simplifying assumption in CMB data analysis is to take the experimental beam response, i.e., the isocontours of constant beam response, to have a perfectly axisymmetric or *circular* shape with a Gaussian profile. This theoretical approximation introduces systematic errors in the statistical analysis at angular scales comparable to the beamwidth, σ. Consistently, it bias estimates probing multipole orders $l \sim 1/\sigma$ in the spherical harmonic analysis (i.e., the generalization of flat-space Fourier analysis for full-sky signals) of CMB experiments.

As far as the main lobe is concerned, experimental beam responses for *off-axis* detectors are well known to exhibit *asymmetric* shapes very well described by an elliptical shape with a Gaussian profile, as discussed for several experiments in the literature, e.g., Planck [1,2], Maxima-1 [3] and Python-V [4]. However, the effect of beam asymmetry has been investigated only recently and the approach taken up to now has relied on semi-analytic [4] or full numerical integration [1,3].

In this paper we shall introduce an analytic approach to address the problem of beam asymmetry in CMB experiments. In particular, we conveniently describe an elliptical Gaussian window in terms of a perturbative expansion around a circular Gaussian one. As it will be shown below, this description allows a simple and intuitive discussion of the beam harmonic transform, the full-sky correlation and covariance matrices for both total intensity and linear polarization anisotropy observations.

The paper is organized as follows: in Sec. II we present our analytic approach and derive the spherical harmonic transform of the total intensity beam. A detailed discussion of the effect of ellipticity to first order is provided in Sec. III. These results are validated numerically in Sec. IV. Results for linear polarization experiments are given in Sec. V. We implement this formalism to calculate full-sky polarization correlation functions in Sec. VI. Errors in temperature and polarization power spectra are discussed in Sec. VII. Finally, we present a general discussion and our main conclusions in Sec. VIII.

II. BEAM SPHERICAL HARMONIC TRANSFORM: TOTAL INTENSITY

Let us consider the beam response, B, to the total intensity sky distribution in a CMB temperature anisotropy experiment. For single-dish experiments with high spatial resolution, the beam geometry can be accurately described in the flat-sky approximation. Within this approximation, an elliptical Gaussian window function can be expressed in Cartesian coordinates,

$$B(x,y) = B_0(\sigma_a,\sigma_b)\exp\left[-\frac{x^2}{2\sigma_a^2}-\frac{y^2}{2\sigma_b^2}\right] \tag{1}$$

where we define σ_a and σ_b as the beam widths in the major (x) and minor (y) axis, and the normalization is given by $B_0(\sigma_a,\sigma_b) = 1/(2\pi\sigma_a\sigma_b)$.

The Fourier transform of the flat-sky elliptical window is simply given by

$$B(k_x,k_y) = \exp\left[-\frac{k_x^2\sigma_a^2}{2}-\frac{k_y^2\sigma_b^2}{2}\right] \tag{2}$$

where k_x and k_y are the modes along the major and minor axis of the ellipse, respectively. However, the Fourier analysis is only accurate for small patches of the sky (i.e., patches covering an area of a few deg^2 or smaller).

For full-sky CMB analysis we shall introduce a decomposition of the window function in the spherical harmonic basis $Y_{lm}(\theta,\phi)$,

*Email address: fosalba@iap.fr
†Email address: dore@iap.fr
‡Email address: bouchet@iap.fr

$$B(\theta,\phi)=\sum_{l}\sum_{m=-l}^{+l} b_{lm}Y_{lm}(\theta,\phi) \tag{3}$$

where $l\approx\pi/\theta$ is the multipole order and b_{lm} are the coefficients of the harmonic transform,

$$b_{lm}=\int d\Omega B(\theta,\phi)Y^{*}_{lm}(\theta,\phi) \tag{4}$$

where $d\Omega=\sin\theta d\theta d\phi$ is the differential solid angle. Above, we have rewritten the elliptical window function $B(\theta,\phi)$ in the (planar) polar coordinates, $x=\theta\cos(\phi-\omega)$ and $y=\theta\sin(\phi-\omega)$,

$$B(\theta,\phi)=B_0\exp\left[-\frac{\theta^2}{2\sigma_b^2}f(\phi)\right] \tag{5}$$

where $f(\phi)\equiv 1-\chi\cos^2(\phi-\omega)$ describes the deviations from a circular (or axisymmetric) Gaussian window and the ellipticity parameter $\chi\equiv 1-(\sigma_b/\sigma_a)^2$ is defined within the range $1>\chi\geqslant 0$. We have introduced an arbitrary phase ω which defines the orientation of the major axis of the elliptical beam in polar coordinates. The circular Gaussian window is thus recovered for the limiting case $\chi=0$.

However, the above integral for the spherical harmonic transform of the elliptical Gaussian window Eq. (4) has no exact analytic solution and one has to resort to semi-analytic approaches or full numerical integration to evaluate it (see, e.g., [4]).

In this section we shall show that Eq. (4) can be solved analytically by introducing a convenient Taylor expansion of the elliptical (non-axisymmetric) window around a circular (axisymmetric) one. This perturbative expansion yields a series in powers of the ellipticity parameter χ,

$$\begin{aligned}B(\theta,\phi)&=B_0\exp\left[-\frac{\theta^2}{2\sigma^2}+\frac{\theta^2}{2\sigma^2}\chi\cos^2(\phi-\omega)\right]\\&\approx B_0\left[B(\theta)+\chi\frac{\theta^2}{2\sigma^2}B(\theta)\cos^2(\phi-\omega)\right]+\mathcal{O}(\chi^2)\end{aligned} \tag{6}$$

where the first term corresponds to a circular Gaussian beam $B(\theta)=\exp[-\theta^2/2\sigma^2]$ of beam width σ_b (the minor axis of the ellipse; we shall denote $\sigma_b=\sigma$ in what follows for simplicity) and $B_0=[\int d\Omega B(\theta,\phi)]^{-1}$ is the beam normalization.

The above expansion of the window function in real space Eq. (6) leads to an analog expansion in harmonic space.

$$b_{lm}=\sum_{n} b^{(n)}_{lm}\frac{\chi^n}{n!}=b^{(0)}_{lm}+b^{(1)}_{lm}\chi+\mathcal{O}(\chi^2) \tag{7}$$

The nth order term of the harmonic transform can be exactly integrated. In particular, only even m modes have a non-vanishing harmonic transform[1] which reads (see Appendix A for the key steps of the derivation),

$$b^{(n)}_{lm}=\frac{2\pi}{2^{2n-m/2}}N_{l-m}\frac{2n!}{(n+m/2)!}\sigma^{2+m}e^{-z}L^{(m)}_{n-m/2}(z) \tag{8}$$

where $z=l^2\sigma^2/2$, N_{lm} is the normalization of the spherical harmonics (see Appendix A) and $L^{(\alpha)}_{\nu}(z)$ denotes the νth order Laguerre polynomials of parameter α [see Eq. (A18) for explicit forms].

Replacing Eq. (8) into Eq. (7) one gets the final expression for the harmonic transform of the elliptical beam

$$b_{lm}=\sigma^m N^I_{lm}e^{-z}\sum_{\nu=0}^{\infty}\gamma_{\nu,m}L^{(m)}_{\nu}(z)\chi^{\nu+m/2}, \tag{9}$$

where we define $N^I_{lm}=N_{l-m}/\overline{B}_0$, $\overline{B}_0=B_0/(2\pi\sigma^2)$, and $\gamma_{\nu,m}=(2\nu+m)!/[2^{2\nu+3m/2}(\nu+m/2)!(\nu+m)!]$. Note that the circular Gaussian beam is recovered when $\chi=0$, in which case only the $m=0$ contribution is non-zero, $b_{lm}=N_{l0}\exp[-l^2\sigma^2/2]\delta_{m,0}$. Combining the conjugation rule for spherical harmonics, $b^{*}_{lm}=(-1)^m b_{l-m}$ (where non-zero m contributors are even for an elliptical beam) and the reality condition of the beam transform, $b^{*}_{lm}=b_{lm}$, one sees that that *both negative and positive modes have the same harmonic transform*, $b_{l-m}=b_{lm}$. Therefore, in what follows, we shall assume $m>0$ without loss of generality.

Equation (9) is one of the main results of this paper. This equation demonstrates that the leading order correction to the circular Gaussian window from a given m mode (for $m>0$) is of order $\mathcal{O}(\chi^{m/2})$. In other words, contributions from higher m modes to the elliptical window function can be identified as higher order corrections to the circular Gaussian window.

For high resolution experiments, $\sigma\ll 1$ rad, *the elliptical beam harmonic transform is dominated by the axisymmetric or circular contribution to the window function*, i.e., the $m=0$ mode. It is important to realize that the circular mode no longer has a Gaussian profile due to ellipticity corrections [see $\nu\neq 0$ terms in Eq. (9)]. To leading order in the small χ expansion [$\nu=0$ in Eq. (9)], contributions from $m>0$ modes are highly suppressed,

$$b_{lm}=\gamma_{0,m}\chi^{m/2}(\sigma l)^m N_{l0}e^{-l^2\sigma^2/2},\quad m=2,4,6,\ldots \tag{10}$$

Therefore non-circular (higher-m) modes only have a non-negligible contribution to the harmonic transform with respect to the circular ($m=0$) mode when $\sigma^2 l^2\approx 1/\chi$, which is well beyond the peak of the window function. The peak of the window is determined from the leading order contribution to b_{l0}, Eq. (12). In fact, the peak location and width can also be accurately estimated from an *effective* circular Gaussian window of width, $\sigma_{eff}=\sigma(1+\chi/4)$,[2]

[1]This is due to the azimuthal symmetry of the elliptical geometry, which is realized in the $\cos^2\phi$ factor of $f(\phi)$ in Eq. (5).

[2]Higher-order corrections in the perturbative expansion, Eq. (9), i.e., higher-order terms in ν and m only modify significantly this definition for very large ellipticities $\chi\simeq 1$.

$$\sigma^2 l_{peak}^2 \simeq (1-\chi/4)/2 \tag{11}$$

since $\chi<1$. Note also that the window function peaks at increasingly higher l multipoles as one considers higher (non-circular) m modes. This is in agreement with recent numerical results [4] and provides a simple demonstration for them.

III. FIRST ORDER ANALYSIS: SLIGHTLY ELLIPTICAL BEAMS

For most current and future experiments, such as Boomerang [5], MAXIMA-1 [6] and Planck [7], the beam is only slightly elliptical, i.e., the widths of the major (σ_a) and minor axis (σ) of the beam differ by less than 20%, $1.2 \geqslant \sigma_a/\sigma \geqslant 1$ ($\chi \leqslant 0.3$).

In this limit, a first order ellipticity correction to the circular Gaussian beam would give an accurate approximation to the actual beam harmonic transform, which yields for the modes $m=0$ and $m=2$,

$$b_{l0} = N_{l0} e^{-l^2\sigma^2/2}\left[1-\frac{\chi}{4} l^2\sigma^2\right] + \mathcal{O}(\chi^2) \tag{12}$$

$$b_{l2} = N_{l0}\frac{\chi}{8} l^2\sigma^2 e^{-l^2\sigma^2/2} + \mathcal{O}(\chi^2) \tag{13}$$

which shows that

$$b_{l2} = \frac{\chi}{8} l^2\sigma^2 b_{l0} + \mathcal{O}(\chi^2) \tag{14}$$

From this equation it is straightforward to see that for $\chi \ll 1$ the leading order contribution from the $m=2$ mode is a few percent of that from $m=0$ at the peak of the window $\sigma^2 l_{peak}^2 \approx 1/2$ [see Eq. (11)].

However, notice that for the circular mode of the window, Eq. (12), *the linear correction to the circular Gaussian window* [the second term in Eq. (12)] *is of the same order and peaks at the same multipole as the leading term in the non-circular* ($m=2$) *mode* [see Eq. (13)]. Therefore, both corrections have to be included to compute the harmonic transform of the elliptical beam consistently. This is illustrated in Fig. 1 for an elliptical beam with $\chi=0.3$ ($\sigma_a/\sigma=1.2$) and $\theta_{\rm FWHM}=10'$.

Similarly, for highly elliptical beams, higher order χ corrections to the circular mode become non-negligible and consequently higher non-circular modes have to be incorporated to calculate the harmonic transform accurately. Explicit expresssions for the window function up to second order in the ellipticity are given in Appendix A, Eq. (A20). This result arises naturally in the perturbative approach to the harmonic analysis of elliptical beams.

IV. NUMERICAL INVESTIGATIONS

In this section we shall validate the analytic results presented in the previous sections regarding the total intensity window. Although the same validation has been carried out for the linear polarization (see Sec. V), we shall concentrate here on the total intensity window as the results for polarization are a straightforward generalization of the total intensity ones.

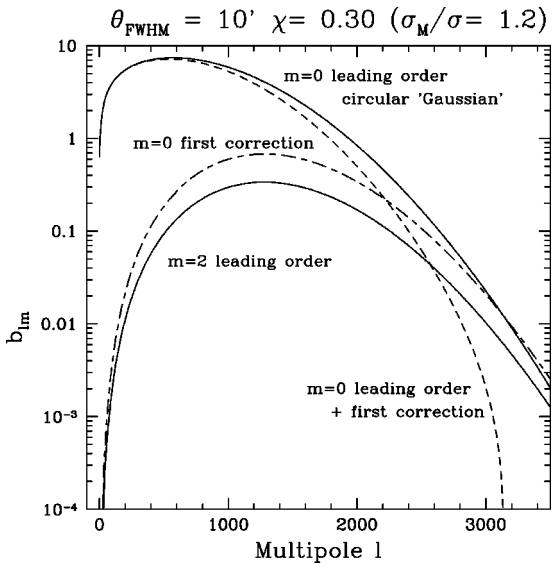

FIG. 1. Ellipticity corrections to the harmonic transform for a slightly elliptical beam, with ellipticity $\chi=0.3$ and resolution $\theta_{\rm FWHM}=10'$. (Solid lines) Leading order terms (for $m=0$ and $m=2$). The first correction to the circular ($m=0$) mode (dashed line) is of the same order and peaks at the same multipole as the leading order term for the non-circular ($m=2$) mode (dot-dashed).

First of all, we shall test whether the perturbative series Eq. (8) is accurate and how fast it converges to the numerical solution. This analysis is done in Sec. IV A. In addition, we shall see in Sec. IV B to what extent the *scaling solution* for the higher m modes of the window, Eq. (10), is a good approximation to the exact solution. As will be discussed in Sec. IV C, prescriptions for an accurate computation of the window function from the perturbative solutions naturally lead to a criteria as to how many higher (non-circular) m modes have to be included in a consistent analysis of elliptical windows.

A. Probing the convergence

To test our approach, we shall compare the analytic results, Eq. (9), to a full numerical integration of Eq. (4) using a Runge-Kutta method of fifth order [8]. The fast convergence of the analytical expansion is illustrated in Fig. 2. Indeed, in this figure we consider for one single beam size, $\theta_{\rm FWHM}=\sqrt{8\ln 2}\sigma=10'$, two different values of the ellipticity parameter, χ: $\chi=0.75$ ($\sigma_a/\sigma=2.0$) and $\chi=0.30$ ($\sigma_a/\sigma=1.2$) shown in the left and right panels, respectively. The upper panels display the expansion $b_{l0}^{(n)}$ for various n. In both situations, the convergence is seen to take place for rather small n. Comparing these two columns we see also that, as expected, the greater the beam ellipticity χ is, the higher the number of terms needed to reach the convergence. Both these statements will be discussed quantitatively below.

The lower panel illustrates this statement by drawing instead the ratio of the individual nth order terms to the 0th

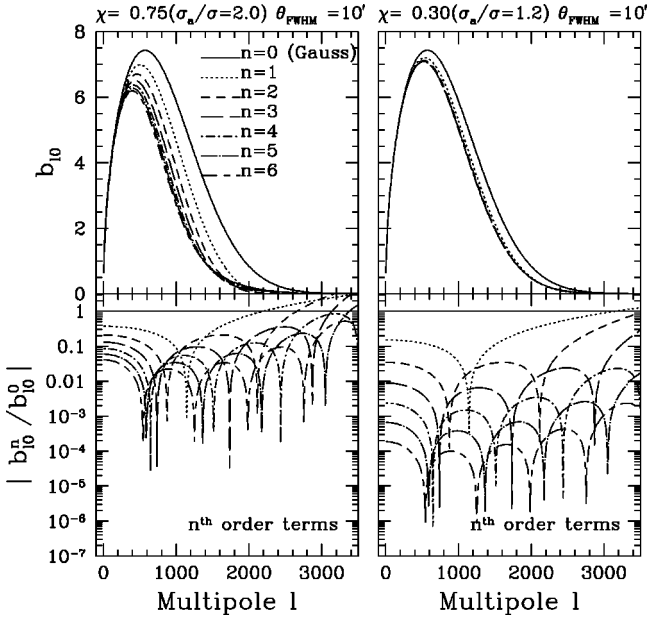

FIG. 2. Probing the convergence. Considering two different ellipticities of a given beam of width $\theta_{\rm FWHM}=10'$, we plot in the upper panel the nth order expansion of b_{lm} and in the lower panel, the ratio of the nth order correction to the 0th one. Both plots illustrate the fast convergence of the χ expansion.

order one (for the same values of n as in the upper panels of Fig. 2).

B. Higher *m* modes contribution

An analogous behavior as the one illustrated above for the $m=0$ mode convergence is seen for $m\neq 0$. We note here that odd m modes are null and that only $m\geqslant 0$ modes are considered since negative modes have exactly the same harmonic transform, $b_{lm}=b_{l-m}$ (see Sec. II). Assuming this convergence, we now examine the amplitude of the higher m modes contribution, as they were derived analytically in Sec. II. This is illustrated in Fig. 3 for a beam of the same width, i.e., $\theta_{\rm FWHM}=10'$, and for 3 different values of χ, namely $\chi=0.17$ $(\sigma_a/\sigma=1.1)$, $\chi=0.30$ $(\sigma_a/\sigma=1.2)$, and $\chi=0.41$ $(\sigma_a/\sigma=1.3)$. We plot here the nth order expansion of b_{lm} for $m=0,2,4$ where n is high enough so that this expansion is fully converged.

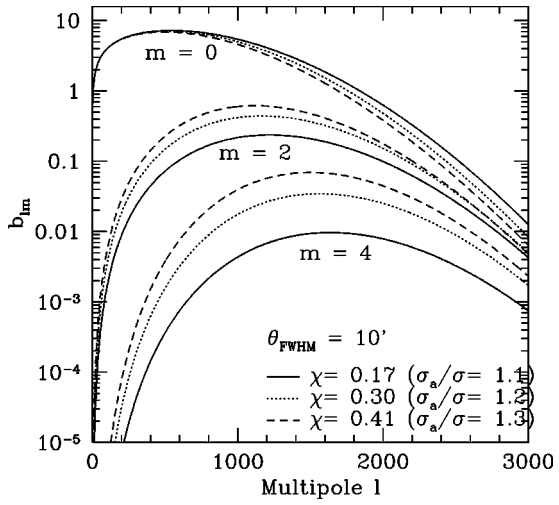

FIG. 3. Higher-m modes in the elliptical window spherical transform.

The scalings demonstrated in Eq. (10) are clearly visible. First we check that $m>0$ modes amplitude scales as $(\sigma l)^m$, making them not only sub-dominant (just a few percent contribution to the beam transform as compared to circular mode $m=0$) but also shifting their peak to higher l as m increases. Second we also check the scaling with the ellipticity, $\chi^{m/2}$, which clearly implies that the smaller χ, the more drastically the $m>0$ modes are suppressed.

A direct comparison with the approximate *scaling solution* for the higher m modes Eq. (10), is shown in Fig. 4. In particular, the plot shows both the fully converged expansion of these $m=0,2,4$ modes and the *scaling solution* for rather small values of the ellipticity χ. We see that both the peak position and the amplitude are pretty well reproduced. Therefore the scaling solution, Eq. (10), is found to be a satisfactory description of such sub-dominant terms in the description of the elliptical beam transform. Note, however, that the larger the beam ellipticity χ, the worse this approximation turns out to be.

C. Prescriptions for an accurate analysis

As was shown above, the convergence of the perturbative development is fast enough so that very few terms of the expansion are needed. To quantify this convergence and to define some useful prescriptions, we compare it to exact nu-

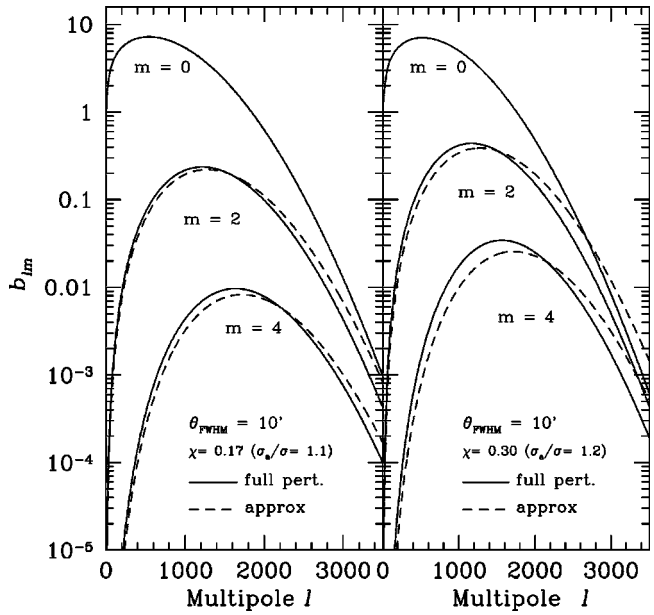

FIG. 4. Probing an approximate computation of b_{lm} for $m=2,4$. Considering one beam of width $\theta_{\rm FWHM}=10'$, we plot both the converged expansion of b_{lm} and an approximate evaluation of it as defined in Eq. (10). The left panel corresponds to $\chi=0.17$ $(\sigma_a/\sigma=1.1)$, and the right one to $\chi=0.30$ $(\sigma_a/\sigma=1.2)$. In both situations, the peak position and its amplitude are well reproduced.

TABLE I. Required number of terms n in the ellipticity expansion, Eq. (8), to achieve a precision greater than 1% up to $l_{max}=5l_{peak}$ for beams of different $\theta_{\rm FWHM}$ and ellipticity χ.

χ (σ_a/σ)		0.17(1.1)	0.30(1.2)	0.40(1.3)	0.49(1.4)	0.55(1.5)
θ_{FWHM}	l_{peak}	548	531	519	509	502
10′	n	2	3	4	6	6
θ_{FWHM}	l_{peak}	1097	1063	1039	1020	1005
5′	n	2	3	4	6	7

merical integration and determine the order n of the b_{l0} expansion needed in order to obtain an agreement better than 1% up to $l_{max}=5l_{peak}$, where l_{peak} denotes the maximum of the window function as defined in Eq. (11). Some prescriptions are summarized in Table I, where we write this order for two different beams of full width half maximum, $\theta_{\rm FWHM}=5'$ and $10'$ and a set of reasonable ellipticities. Even if we see that naturally the greater the ellipticity, the greater is the required n, as a matter of fact, in most of practical situations (see Sec. VIII), 3 terms at most are needed.

Note that this criteria is very stringent and if we require, say, only a 2% accuracy at the peak level, only 1 ellipticity correction is needed for $\chi\leqslant 0.3$, i.e., $\sigma_a/\sigma\leqslant 1.2$.

The numbers presented in this table lead to another requirement. Indeed, as was discussed in Sec. III the nth order correction to the $m=0$ mode is of the same order as the leading order contribution to the $m=n$ mode (m even) [see Eqs. (9) and (10)]. Thus to be self-consistent, *the highest perturbative order, n, in the ellipticity corrections to the circular* ($m=0$) *mode of the window, b_{l0}, should match the highest-m mode considered for an accurate computation of the full beam transform, b_{lm}*. For example, Table I implies that to handle properly the elliptical beam effects at a 1% precision till $l_{max}=5l_{peak}$, e.g., for a beam of $\theta_{\rm FWHM}=10'$, we have to include $m=2$ mode for $\chi=0.17$ or 0.30, while one has to include $m=2,4$ modes for $\chi=0.40$, and so forth.

V. BEAM SPHERICAL HARMONIC TRANSFORM: LINEAR POLARIZATION

The CMB radiation is expected to be linearly polarized as caused by Thomson scattering of CMB photons off hot electrons primarily at the surface of last scattering (see [9–12]) while the foreground Galactic emission is observed to be linearly polarized as well (see, e.g., [13] for recent reviews and references therein). Thus we shall focus here on the detection of linearly polarized radiation and neglect circular polarization in what follows.

The case for a linearly polarized beam with an elliptical shape can be treated in an analog way to the formalism developed in Sec. II for the total intensity beam.

Linearly polarized radiation can be conveniently described in terms of the so-called Stokes parameters, $\tilde{Q}$ and $\tilde{U}$ (note that we use $\tilde{X}$ to denote beam parameters, as opposed to sky parameters, X). Stokes parameters of a plane wave are related to the amplitudes of the electric field of the wave in two directions orthogonal to the wave propagation direction.

Following standard notation (see, e.g., [14–18]), the Stokes parameters of the beam are decomposed in the spin-2 spherical harmonics basis ${}_{\pm 2}Y_{lm}$ as

$$\frac{1}{\sqrt{2}}(\tilde{Q}\pm i\tilde{U})=\sum_{lm}\,(b^G_{lm}\mp ib^C_{lm})_{\mp 2}Y_{lm} \tag{15}$$

Equivalently, the harmonic transform of a linearly polarized beam in terms of the so-called gradient "G" and curl "C" components reads

$$b^G_{lm}\pm ib^C_{lm}=\frac{1}{\sqrt{2}}\int d\Omega(\tilde{Q}\mp i\tilde{U})_{\pm 2}Y^*_{lm} \tag{16}$$

from which it follows that

$$b^G_{lm}=\frac{1}{2\sqrt{2}}\int d\Omega[(\tilde{Q}-i\tilde{U})_2Y^*_{lm}+(\tilde{Q}+i\tilde{U})_{-2}Y^*_{lm}],$$

$$b^C_{lm}=\frac{-i}{2\sqrt{2}}\int d\Omega[(\tilde{Q}-i\tilde{U})_2Y^*_{lm}-(\tilde{Q}+i\tilde{U})_{-2}Y^*_{lm}] \tag{17}$$

where the above expressions assume that the available power to each of the modes (G,C) is 1/2 of the total intensity (i.e., we assume fully polarized detectors, with no sensitivity to circular polarization). Note that this G (gradient) and C (curl) components of the linear polarization are simply linked to the E and B ones, respectively, in the following way,

$$b^E_{lm}=-\sqrt{2}b^G_{lm},\quad b^B_{lm}=-\sqrt{2}b^C_{lm}; \tag{18}$$

See [19] for a pedagogical discussion of the E,B polarization modes. For a pure co-polar beam (i.e., for an ideal optical system and telescope, see [18]), we have

$$\tilde{Q}\pm i\tilde{U}=-B(\theta,\phi)e^{\pm 2i\phi} \tag{19}$$

where $B(\theta,\phi)$ is defined as in Eq. (5). Equation (19) reflects the spin-2 nature of linear polarization in the (θ,ϕ) basis.

Let us evaluate the harmonic transform of the linearly polarized beam. Using the parity symmetries for an elliptical beam (see Appendix B),

$$b^C_{lm}=ib^G_{lm},\quad b^C_{l-m}=-ib^G_{l-m} \tag{20}$$

and the general (intrinsic to the definition of the G,C components) parity transformations,[3]

$$b^P_{l-m}=b^P_{lm}, \quad P=G,C \tag{21}$$

one realizes that the harmonic transform of linear polarization can be fully determined from one of the two components alone, say G. Moreover, both negative and positive modes have the same harmonic transform. Thus, in what follows, we shall assume $m\geqslant 0$ without loss of generality.

In full analogy with the total intensity computation (see Sec. II) we introduce a perturbative expansion of the elliptical beam,

$$b^G_{lm}=\sum_n b^{G(n)}_{lm}\frac{\chi^n}{n!}=b^{G(0)}_{lm}+b^{G(1)}_{lm}\chi+\mathcal{O}(\chi^2). \tag{22}$$

This expansion can be exactly integrated for any order in an analogous way to the total intensity case and yields (see Appendix B for the basic steps of the computation),

$$b^G_{lm}=\sigma^{m-2}N^G_{lm}e^{-z}\sum_{\nu=0}^{\infty}\gamma_{\nu,m-2}L^{(m-2)}_{\nu}(z)\chi^{\nu+m/2-1} \tag{23}$$

where we define $N^G_{lm}=-l^{2m}M_{lm}/(4\sqrt{2}\overline{B}_0)$, and the coefficients $\gamma_{\nu,m-2}$ are the same as those defined for the total intensity Eq. (8). The normalization M_{lm} is given in Appendix B along with the basic notation for the spin-2 harmonics.

Note that, up to the normalization N^G_{lm}, the linear polarization beam transform Eq. (23) is formally the same as the total intensity one, Eq. (8), with the index for the m modes shifted by $m\rightarrow m-2$. This shift is introduced by the difference in the spin index s between the linearly polarized beam $s=2$ [see Eq. (19)] and the total intensity beam $s=0$.

In particular, Eq. (23) shows that *the $m=2$ mode dominates the harmonic transform of the linearly polarized elliptical beam*. Note that for a circular Gaussian beam ($\chi=0$) *only* the $m=2$ mode is non-vanishing. To leading order in the ellipticity expansion [$\nu=0$ in Eq. (23)] one finds that contributions from $m>2$ modes are subdominant:

$$b^G_{lm}=-\gamma_{0,m-2}\chi^{m/2-1}(\sigma l)^{m-2}\frac{N_{l0}}{2\sqrt{2}}e^{-l^2\sigma^2/2} \tag{24}$$

with $m=4,6,\ldots$. In particular, one finds the same suppression of higher m modes with respect to $m=2$, in full analogy to the results for the total intensity Eq. (10). Also, the linear polarization window function peaks at increasingly higher l multipoles as one considers higher m modes, as was the case for the total intensity window.

The expressions for the first non-zero m contributors ($m=2$ and $m=4$ modes) up to the first ellipticity correction are

$$b^G_{l2}=-\frac{N_{l0}}{2\sqrt{2}}e^{-l^2\sigma^2/2}\left[1-\frac{\chi}{4}l^2\sigma^2\right]+\mathcal{O}(\chi^2) \tag{25}$$

$$b^G_{l4}=-\frac{N_{l0}}{2\sqrt{2}}\frac{\chi}{8}l^2\sigma^2e^{-l^2\sigma^2/2}+\mathcal{O}(\chi^2) \tag{26}$$

and therefore,

$$b^G_{l4}=\frac{\chi}{8}l^2\sigma^2b^G_{l2}+\mathcal{O}(\chi^2) \tag{27}$$

and the same expressions hold for negative modes, as $b^G_{l-m}=b^G_{lm}$. This is in full analogy with the scaling relation between higher m modes found for the total intensity window, Eq. (14).

Whenever the beam ellipticity is fairly large, one has to consider higher-order corrections in the ellipticity to compute accurately the window function. Explicit expresssions for the window function up to *second order* in the ellipticity are given in Appendix B, Eq. (B22).

VI. FULL-SKY POLARIZATION CORRELATION MATRIX

Linearly polarized radiation is described by the total intensity T and the Stokes parameters Q and U. If the CMB polarized radiation is Gaussian distributed, one needs, *a priori*, six statistical quantities to characterize correlations among them. It is more convenient to use linear combinations of the Stokes parameters with different parity properties, the so-called E (or gradient G) and B (or curl C) modes, for which only four correlations are non-vanishing. Namely the correlation between E and T modes and the three autocorrelations.

Following [21] we will consider the correlation matrix $\mathbf{M}$ between two arbitrary measurements in the sky

$$\mathbf{M}(\hat{\mathbf{n}}_1,\hat{\mathbf{n}}_2)\equiv\begin{pmatrix}\langle T_1T_2\rangle & \langle T_1Q_2\rangle & 0\\ \langle T_1Q_2\rangle & \langle Q_1Q_2\rangle & 0\\ 0 & 0 & \langle U_1U_2\rangle\end{pmatrix} \tag{28}$$

where 1,2 denote the directions $\hat{n}_1,\hat{n}_2$ in the sky. The cross terms $\langle T_1U_2\rangle=\langle Q_1U_2\rangle=0$ as required by symmetry under parity transformations (see, e.g., [17]).

The entries of the correlation matrix are defined as follows:

$$\langle P_1P_2\rangle=\langle P^*_{eff}(\hat{n}_1,\omega_1)P_{eff}(\hat{n}_2,\omega_2)\rangle,$$

$$P_{eff}(\hat{n},\omega)=\int d\Omega D(\phi,\theta,\omega)\tilde{P}^*P \tag{29}$$

where P_{eff} is the result of convolving the polarized beam $\tilde{P}=\tilde{T},\tilde{Q},\tilde{U}$ with the sky, $P=T,Q,U$.

In this formalism the "scanning strategy" of a given experiment is obtained by specifying the Euler angles as a function of time t, $(\phi(t),\theta(t),\omega(t))$, where $\hat{n}=\hat{n}(\theta(t),\phi(t))$ gives the pointing direction of the beam and

[3]Note that these conjugation rules are consistent with [17] and [20], and are inconsistent by a factor $(-1)^m$ with respect to [21].

$\omega(t)$ is the rotation angle around the pointing direction $\hat{n}$ which specifies the orientation of an asymmetric beam (e.g., the major axis orientation for an elliptical Gaussian beam) with respect to a fix reference orientation [e.g., $\omega(t=0)$].

Accordingly, the rotation operator $D(\phi,\theta,\omega)$ acts on the beam so that it takes all possible orientations with respect to a fix reference frame in the sky [22,18]. Simple scanning strategies allow a convenient decomposition of the rotation matrix $D(\phi(t),\theta(t),\omega(t))$ for the implementation of fast methods to compute the full-sky convolution [22,18]. In what follows we shall suppress the time dependence of the Euler angles to simplify notation.

Decomposing the polarization field in spin harmonics one finds the following expressions for the Stokes parameters of the beam convolved with the sky [see Eq. (5) of [22] and Eq. (39) of [18]]:

$$T_{eff}=\sum\ [D^{l}_{mM}(\phi,\theta,\omega)]^{*}b^{*}_{lM}a_{lm} \tag{30}$$

$$Q_{eff}=2\sum\ [D^{l}_{mM}(\phi,\theta,\omega)]^{*}b^{G*}_{lM}a^{G}_{lm} \tag{31}$$

$$U_{eff}=2\sum\ [D^{l}_{mM}(\phi,\theta,\omega)]^{*}b^{G*}_{lM}a^{C}_{lm} \tag{32}$$

where we define $a^{G}_{lm}=(a_{2,lm}+a_{-2,lm})/2\sqrt{2}$ and $ia^{C}_{lm}=(a_{2,lm}-a_{-2,lm})/2\sqrt{2}$.

Note that for the linear polarization parameters Q,U, an overall factor of 2 accounts for the fact that both G and C modes contribute equally to the transform of an elliptical beam.

The polarization correlation matrix can be easily computed making use of symmetry properties of the rotation matrices and the addition theorem of rotations (see Appendix C),

$$\langle T_1T_2\rangle=\sum_{l}\ b^{TT}_{l}C^{T}_{l} \tag{33}$$

$$\langle T_1Q_2\rangle=2\sum_{l}\ b^{TG}_{l}C^{TG}_{l} \tag{34}$$

$$\langle T_1U_2\rangle\propto C^{TC}_{l}=0 \tag{35}$$

$$\langle Q_1U_2\rangle\propto C^{GC}_{l}=0 \tag{36}$$

$$\langle Q_1Q_2\rangle=4\sum_{l}\ b^{GG}_{l}C^{G}_{l} \tag{37}$$

$$\langle U_1U_2\rangle=4\sum_{l}\ b^{GG}_{l}C^{C}_{l} \tag{38}$$

where we have used the fact that $C^{TC}_{l}=C^{GC}_{l}=0$ as follows from the general property that the T,G harmonic coefficients of a field transform differently under parity than the C harmonics. The power spectra are defined as

$$\langle a^{P*}_{lm}a^{P}_{l'm'}\rangle=C^{P}_{l}\delta_{ll'}\delta_{mm'},\quad P=T,G,C \tag{39}$$

and we have introduced the "2-point window functions"

$$b^{PP'}_{l}=\sum_{MM'}\ D^{l}_{M'M}b^{P*}_{lM}b^{P'}_{lM'},\quad P=T,G \tag{40}$$

where hereafter we drop the tilde to denote beam quantities (i.e., we take $\tilde{P}\to P$) to ease notation. We note that the first non-vanishing contributions to the total intensity $b^{T}_{lm}=b_{lm}$ enter at $m=0$, while linear polarization beams b^{G}_{lm} have the first non-zero contributor from $m=2$.

The rotation matrix $D^{l}_{M'M}$ above reads [see Eq. (2) in Sec. 4.7.1 and Eq. (5) in Sec. 4.7.2 of [23]]

$$D^{l}_{M'M}(\alpha-\omega_2,\beta,\gamma-\omega_1)=d^{l}_{M'M}(\beta)e^{-i[M'(\alpha-\omega_2)+M(\gamma-\omega_1)]} \tag{41}$$

where the Euler angles (α,β,γ) of the resulting rotation matrix are [Eq. (6) in Sec. 4.7.2 of [23]; see also [4]],

$$\begin{aligned}\cot\alpha&=\cos\theta_2\cot(\phi_1-\phi_2)-\cot\theta_1\sin\theta_2\csc(\phi_1-\phi_2)\\ \cos\beta&=\cos\theta_1\cos\theta_2+\sin\theta_1\sin\theta_2\csc(\phi_1-\phi_2)\\ \cot\gamma&=\cos\theta_1\cot(\phi_1-\phi_2)-\cot\theta_2\sin\theta_2\csc(\phi_1-\phi_2)\end{aligned} \tag{42}$$

and the orientation of the beam at pixels 1 and 2 is given by ω_1 and ω_2. The *irreducible* rotation matrices [see Eq. (2.17) of [24] and Eq. (4) in Sec. 4.3.1 of [23]] read

$$d^{l}_{nm}(\beta)=\sum_{t}\ (-1)^{t}\frac{[(l+n)!(l-n)!(l+m)!(l-m)!]^{1/2}}{t!(l+n-t)!(l-m-t)!(t+m-n)!}\times(\cos\beta/2)^{2l+n-m-2t}(\sin\beta/2)^{2t+m-n} \tag{43}$$

where t is summed up for all values which yield non-negative factorials. These matrices give the dependence of the polarization correlation functions on the separation (or lag) angle in the sky $\beta=\hat{n}_1\cdot\hat{n}_2$. Thus, predictions for the polarization correlation matrix for cosmological models of the sky signal convolved with an elliptical window assuming a particular scanning strategy are given by Eqs. (9), (23), (42), and (43). The polarization correlation matrix thus obtained can be used to compute the likelihood functions and the Fisher information matrix for a given sky realization of a cosmological model convolved with an elliptical beam.

Slightly elliptical beams

Provided the beam ellipticity is small ($\chi\ll 1$) a first order ellipticity correction to the circular Gaussian beam yields a good approximation to the elliptical beam transform (see Sec. III). Consistently, one can expand the polarization correlation functions to first order in the ellipticity expansion.

For this purpose, first we need to write out explicitly the first terms of the 2-point window,

$$b^{PP'}_{l}=D^{l}_{00}b^{P}_{l0}b^{P'}_{l0}+D^{l}_{02}b^{P}_{l0}b^{P'}_{l2}+\cdots \tag{44}$$

where we have taken the real part of the 2-point function as we want to compute the polarization correlation functions that are observable and therefore real. Equation (44) for the case of the total intensity ($P=T$) is in agreement with Eq. (33) in [14]. Introducing the expansion of the (1-point) windows b^P_{lm} to first order in the ellipticity Eqs. (12), (13), (25), and (26) into Eq. (44) one obtains the following expressions for the correlation functions:

$$\langle T_1 T_2\rangle = \sum_l C_l^T \left[D^l_{00} + \frac{\chi}{2} l^2\sigma^2 (D^l_{02} - D^l_{00}) \right] \left(\frac{2l+1}{4\pi} \right) e^{-l^2\sigma^2} + \mathcal{O}(\chi^2) \tag{45}$$

$$-\langle T_1 Q_2\rangle = \sqrt{2}\sum_l C_l^{TG} \left[D^l_{02} + \frac{\chi}{8} l^2\sigma^2 (D^l_{04} + D^l_{22} - 4D^l_{02}) \right] \times \left(\frac{2l+1}{4\pi} \right) e^{-l^2\sigma^2} + \mathcal{O}(\chi^2) \tag{46}$$

$$\langle Q_1 Q_2\rangle = \sum_l C_l^G \left[D^l_{22} + \frac{\chi}{4} l^2\sigma^2 (D^l_{24} - 2D^l_{22}) \right] \left(\frac{2l+1}{4\pi} \right) e^{-l^2\sigma^2} + \mathcal{O}(\chi^2) \tag{47}$$

$$\langle U_1 U_2\rangle = \sum_l C_l^C \left[D^l_{22} + \frac{\chi}{4} l^2\sigma^2 (D^l_{24} - 2D^l_{22}) \right] \left(\frac{2l+1}{4\pi} \right) e^{-l^2\sigma^2} + \mathcal{O}(\chi^2) \tag{48}$$

where the sum involving the rotation matrices $D^l_{MM'}$ is restricted to $l \geq M + M'$, and

$$\begin{aligned}
D^l_{00} &= d^l_{00}(\beta) = P_l(\cos\beta) \\
D^l_{02} &= d^l_{02}(\beta)[\cos 2\alpha + \cos 2\gamma] \\
D^l_{22} &= d^l_{22}(\beta)\cos 2(\alpha+\gamma) \\
&\quad + (-1)^l d^l_{22}(\pi-\beta)\cos 2(\alpha-\gamma) \\
D^l_{04} &= d^l_{04}(\beta)[\cos 4\alpha + \cos 4\gamma] \\
D^l_{24} &= d^l_{24}(\beta)[\cos(2\alpha+4\gamma) + \cos(4\alpha+2\gamma)] \\
&\quad + (-1)^l d^l_{24}(\pi-\beta)[\cos(2\alpha-4\gamma) + \cos(4\alpha-2\gamma)]
\end{aligned} \tag{49}$$

where we have to replace $\alpha \to \alpha - \omega_2, \gamma \to \gamma - \omega_1$ to introduce the beam orientation in the above equations, as determined by Eq. (41). We have used the symmetry properties of the *d*-rotation matrices [see Sec. 4.4, Eq. (1), in [23]]

$$d_{MM'}(\beta) = (-1)^{M'-M} d_{MM'}(\beta),$$

$$d_{M-M'}(\beta) = (-1)^{l+M} d_{MM'}(\pi-\beta),$$

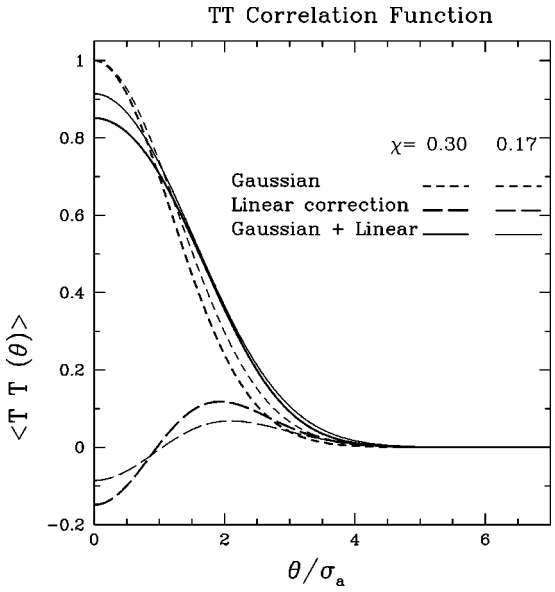

FIG. 5. Temperature correlation function for a slightly elliptical beam. It assumes a flat power spectrum, $C_l = \text{const}$. (Short dashed line) Correlation function for a circular Gaussian beam. (Long dashed line) Linear ellipticity correction assuming the beam scans the sky in ecliptic latitude and a fixed beam orientation in the sky. (Solid) Total correlation function (Gaussian + linear correction). Thick lines assume $\chi = 0.3$ ($\sigma_a/\sigma = 1.2$) while thin lines correspond to $\chi = 0.17$ ($\sigma_a/\sigma = 1.1$).

and the reality condition on the correlations functions. The *irreducible* d_{sm} matrices can be expressed in terms of Legendre polynomials by relating the previous to the spin-*s* harmonics [see Eqs. (3.4), (3.11) in [25]],

$$d^l_{sm}(\beta) = \sqrt{\frac{4\pi}{2l+1}}\, {}_{-s}Y_{lm}(\beta, 0) \tag{50}$$

For $s = 0,2$ one gets [see Eqs. (A4) and (B2)],

$$\begin{aligned}
d^l_{0m}(\beta) &= \sqrt{\frac{(l-m)!}{(l+m)!}} P^m_l(\cos\beta), \\
d^l_{2m}(\beta) &= 2\sqrt{\frac{(l-2)!(l-m)!}{(l+2)!(l+m)!}}\, {}_{-2}P^m_l(\cos\beta)
\end{aligned} \tag{51}$$

and ${}_{-2}P^m_l(\cos\beta)$ are given in Eq. (B4). This explicitly shows that the ellipticity (asymmetry) of the window function introduces a dependence of the correlation functions on the scanning strategy, as parametrized by the angles (α, β, γ). We stress that the above equations are appropriate for a full-sky analysis, since the small-angle approximation is only taken for the beam geometry (which is of small extent in radians).

In Fig. 5 we display the temperature correlation function $\langle TT\rangle$ (we drop sub-indices labeling sky pixels to ease notation) for a slightly elliptical beam Eq. (33). We assume a flat power spectrum, $C_l = \text{const}$. This allows us to emphasize the effect of the window function irrespective of the underlying cosmological model assumed. For the case shown in Fig. 5

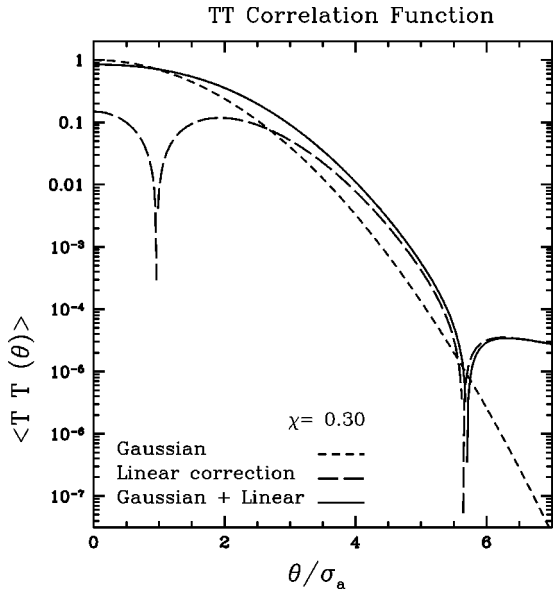

FIG. 6. Same as Fig. 5 but for the absolute value of the correlations in logarithmic scale to emphasize small residual correlations induced by the beam at large angular separations. Only lines for an ellipticity of $\chi=0.3$ are shown for clarity.

we assume that the telescope scans the sky in ecliptic latitude (i.e., $\alpha=\gamma=0$) and that the beam hits a given sky pixel always with the same orientation (i.e., we consider correlated pixels for beams aligned in the sky) which provides an upper limit to the effect of ellipticity on the correlation functions. This is because scanning strategies that observe a given sky pixel with a different orientation of the beam each time it scans over it tend to average out the impact of beam asymmetry on full-sky estimators.

As seen in the plots, the linear ellipticity correction to the circular Gaussian window introduces an anti-correlation for pixels separated by $\theta \leqslant \sigma_a$ (the major axis beam width). This

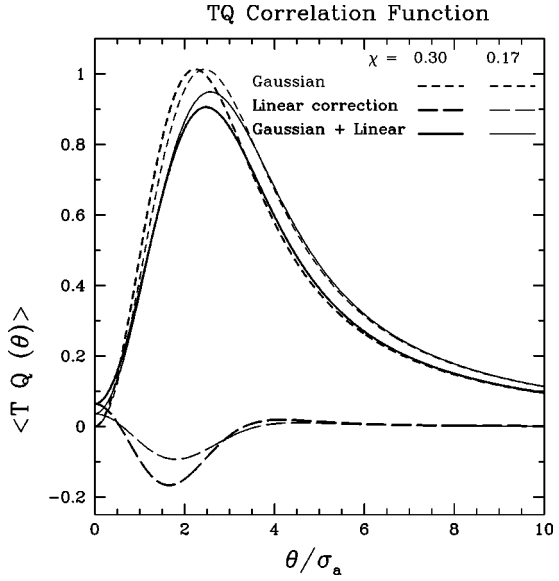

FIG. 7. Cross-correlation temperature polarization. Conventions are the same as in Fig. 5.

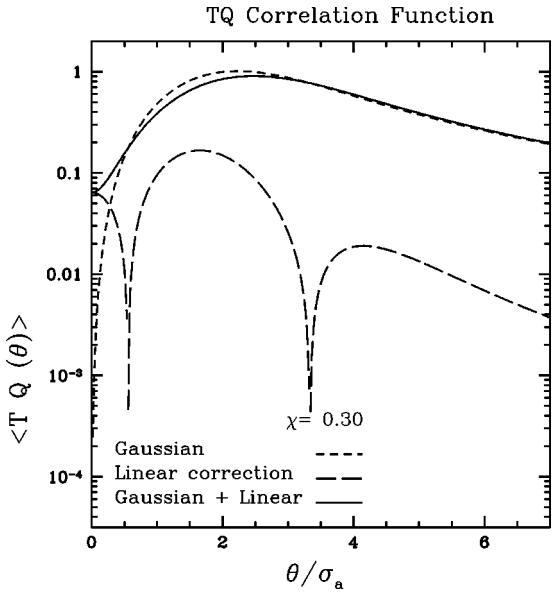

FIG. 8. Same as Fig. 7 but in logarithmic scale.

is because pixels within this angular separation are seen as a single *smeared pixel*. Alternatively, for $\theta \geqslant \sigma_a$ the ellipticity increases the correlation between sky pixels. This correlation peaks at $\theta=2\sigma_a$, where it yields a 20% correction (for $\chi=0.3$) to the Gaussian correlation function and decreases monotonously for larger distances, as expected. However, a closer look (see Fig. 6) reveals that some small residual anti-correlations induced by the ellipticity (at the level of 10^{-5}) remain at large distances which might be a reflection of the limitations of a linear order analysis. Non-linear terms in the ellipticity expansion are expected to cancel out these long-range correlations.

Cross correlations for temperature polarization and linear polarization auto-correlation functions are shown in Figs. (7),(8), and (9),(10), respectively. In particular, we see that the effect of ellipticity is comparable for the temperature auto-correlation $\langle TT \rangle$ and cross-correlation functions $\langle TQ \rangle$ (at most a 15% correction to the Gaussian correlation for $\chi=0.3$), while tends to be less significant for the linear polarization $\langle QQ \rangle$ (just a few percent correction). Notice that the angular scale for the transition between negative and positive ellipticity-induced correlations (first and second bumps in the logarithmic scale plots) is shifted in the correlations involving linearly polarized windows with respect to the case for the temperature (or total intensity) discussed above (see Figs. 5 and 6).

VII. COVARIANCE MATRIX

In this section we shall discuss the covariance of the power spectra for elliptical beams in the presence of uncorrelated[4] noise, following the standard formalism developed for circular windows [26] (see also

[4]The noise is assumed to be uncorrelated between different pixels and between temperature and linear polarization measurements.

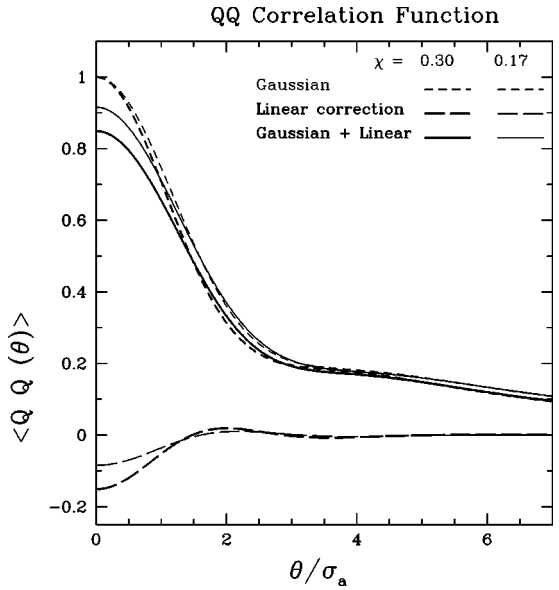

FIG. 9. Linear polarization correlation function in terms of the Stokes Q parameter. Note that for the case shown (a flat power spectrum), $\langle QQ\rangle=\langle UU\rangle$. Conventions are the same as in Fig. 5.

[16,17,15, 27,21,20]). In particular, we shall use this formalism to estimate error bars for the power spectra for elliptical window functions. For this purpose we shall assume that the circular mode of an elliptical window, which has a *non-Gaussian* profile, yields an approximately unbiased estimate of the actual error bars, as we shall argue below.

The covariance of the temperature power spectrum C_l^T can be easily computed for the circular mode ($m=0$) of the window function [26]

$$\Delta(C_l^T)=\sqrt{\frac{2}{(2l+1)\Delta l f_{sky}}}[C_l^T+w^{-1}(b_{l0})^{-2}]. \quad (52)$$

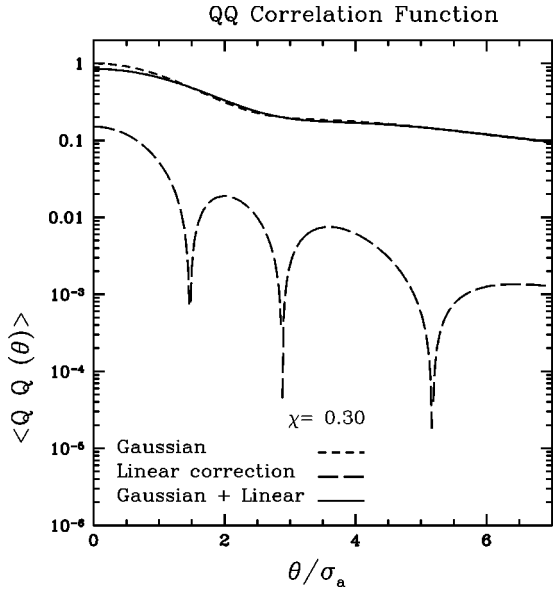

FIG. 10. Same as Fig. 9 but in logarithmic scale.

Similarly for linear polarization, one obtains from the lowest m-mode contribution ($m=\pm 2$) [17,27],

$$\Delta(C_l^P)=\sqrt{\frac{2}{(2l+1)\Delta l f_{sky}}}[C_l^P+w^{-1}(2b_{l2}^G)^{-2}] \quad (53)$$

where $P=G,C$, and for the cross-spectra

$$\Delta(C_l^{TG})=\sqrt{\frac{1}{(2l+1)\Delta l f_{sky}}}\{(C_l^{TG})^2+[C_l^T+w^{-1}(b_{l0}^T)^{-2}] \times[C_l^G+w^{-1}(2b_{l2}^G)^{-2}]\}^{1/2} \quad (54)$$

where the factor of 2 in the polarization windows accounts for equal contributions from $m=\pm 2$. The factors Δl and f_{sky} in the above expressions account for the binning in l space used (we assumed $\Delta l=75$ for all experiments) and the fraction of the sky observed by the experiment, respectively. The weight per solid angle is $w\equiv(\sigma_{pix}^2\omega_{pix})^{-1}$ while the noise per pixel $\sigma_{pix}=s/\sqrt{t_{pix}}$ depends on the detector sensitivity s and the observing time per pixel t_{pix}. The pixel solid angle $\omega_{pix}=\theta_{\rm FWHM}\times\theta_{\rm FWHM}$. The above expressions for the noise associated with the power spectra estimation, Eqs. (52)–(54), assume that all detectors in the experiment have the same noise properties and main beam response.

Note that polarization power spectra have twice as much noise per pixel as the temperature spectrum since only half of the total power is available to each polarization mode (G and C). This is accounted for through the normalization of the window functions [see factor $\sqrt{2}$ in Eq. (16)].[5]

We stress that the above expressions only include the leading order in the m-mode expansion of the elliptical window. However, this is a good approximation to (i.e., it is the dominant term in) the exact window function for elliptical beams as discussed in Sec. III. In principle, this analysis could be rigorously extended to include higher m modes of the window by computing the a_{lm}'s of the sky map convolved with the elliptical window, from which the power spectra of the convolved map and their associated errors can be calculated (see Appendix A.2 in [28]). However, thorough numerical analyses ([3]; see also [1]) we show that an azimuthally symmetrized component of the window yields an unbiased estimate of the power spectrum within a few percent, which suggests that non-circular modes of the window function can be safely neglected, at least for slightly elliptical beams.

Predictions for the theoretical error bars for the temperature power spectrum for current CMB experiments are shown in Fig. 11. Experimental parameters are taken from [29,30] (MAXIMA-1), [31,32] (Boomerang), [33] (Archeops) and [34] (Planck). The figures used correspond to averages among channels and they only intend to be illustrative. Note that for Archeops and Planck the experimental numbers given are just nominal. It is seen that the pixel noise enlarges the error bars at multipoles $l\approx 1000$, except for the

[5]Alternatively, one can define different pixel weights w for temperature and linear polarization, $w^P=2w^T$ (see, e.g., [17])

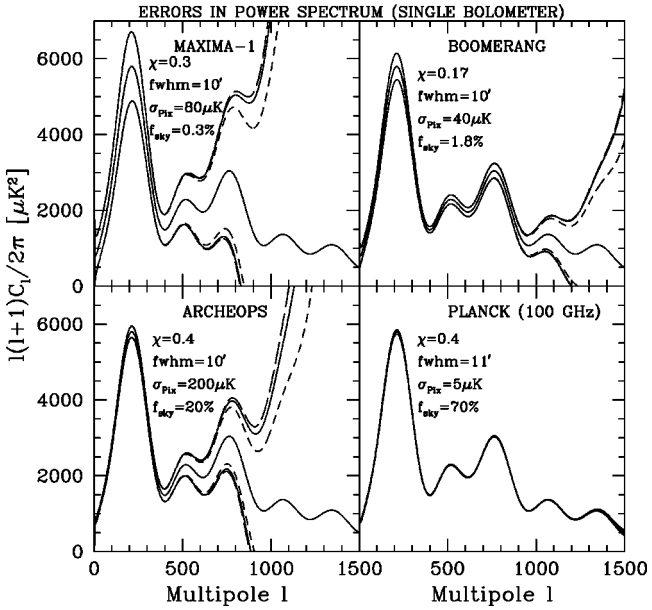

FIG. 11. Errors in the power spectrum estimation for current and future experiments. It assumes an underlying standard Λ CDM model. Pairs of lines (above and under the mean power spectrum) show different estimates for the theoretical error bars according to different choices of the window function: short-dashed lines are predictions for a circular Gaussian window of beam width given by the minor axis of the ellipse σ, solid lines correspond to the elliptical window to first order, Eq. (12), while long-dashed lines are obtained from an *effective circular Gaussian window* of beam width $\sigma_{eff}=\sqrt{\sigma_a \sigma}$, where σ_a is the major axis of the ellipse. In all cases, a binning in l space is used of width $\Delta l=75$.

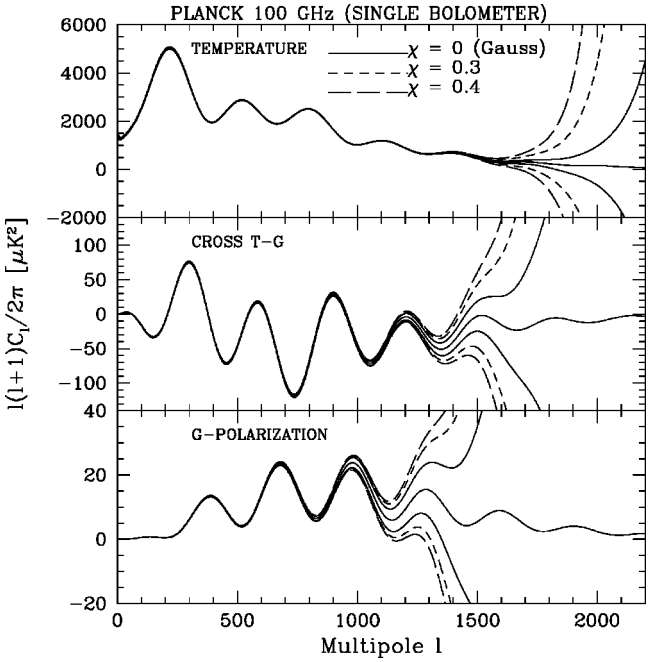

FIG. 12. Errors in the power spectrum estimation from a single 100 GHz detector of the Planck satellite. It assumes the same experimental parameters as those given in Fig. 11 (bottom right panel). Solid lines show the mean theoretical power spectra and their error bars for realizations of the sky convolved with a Gaussian beam. Dashed lines show the analog error bars for the case of an elliptical beam. The upper panel displays the temperature anisotropy power spectrum, the middle panel shows the cross temperature polarization (in terms of the G mode), while the bottom panel corresponds to the polarization (G mode).

Planck satellite experiment. Main differences between error forecasts for different experiments are due to the sky coverage and noise per pixel (for a single channel). It is also observed that the error bars computed for a Gaussian window underestimate those of an elliptical window [computed according to Eq. (12)]. However, to first order the error bars for an elliptical beam can be well approximated by using an *effective Gaussian window* of the form $b_{l0}=\exp[-l^2\sigma_a\sigma/2]$, where σ_a and σ are the major and minor axes of the ellipses of a constant beam response.

A detailed analysis of the expected error bars in the power spectra estimation, including polarization for the Planck satellite (single 100 GHz channel), is summarized in Fig. 12. As discussed above, the high sensitivity of the Planck satellite allows a clean recovery of the CMB power spectra up to $l \gtrsim 1000$ with a single channel data (except for the C-polarization mode, see below). In fact, pixel noise starts enlarging the error bars for the temperature anisotropy power spectrum at $l \gtrsim 1500$ (see the upper panel in Fig. 12). For the cross-spectrum temperature polarization (G mode) one finds that pixel noise becomes dominant at $l \gtrsim 1000$ (see the middle panel) whereas for polarization (G mode), this happens at lower multipoles $l \approx 1000$ (see the lower panel). We have checked (although this is not shown in Fig. 12 for the sake of clarity) that for the polarization C mode error bars become pixel-noise dominated at $l \lesssim 500$ as the signal is typically (i.e., for standard CDM models) found at a few percent level of that in the G mode.

Beyond these multipoles (i.e., for smaller scales) the effect of the ellipticity of the window becomes significant. Moreover, using a circular Gaussian window clearly underestimates error bars for elliptical beams approximately computed according to Eqs. (12) and (25) for the total intensity and linear polarization windows, respectively.

VIII. DISCUSSION

As cosmic microwave background (CMB) experiments image the sky at finer spatial resolution with higher sensitivity, new relevant systematic effects have to be properly taken care of in the process of data analysis in order to consistently extract cosmological information down to the smallest scales probed by the experiment. The asymmetry of the beam response is becoming an increasingly important issue which has been largely neglected until recently in CMB studies.

In this paper we have introduced an analytic approach to describe the effect of beam ellipticity in CMB experiments. This approach is based on a perturbative expansion around the geometry of a circular Gaussian beam, which yields a series expansion of the elliptical Gasusian beam in powers of the ellipticity parameter. There are several advantages of introducing a perturbative approach to discuss beam ellipticity.

It provides a simple and convenient way of integrating the beam harmonic transform for the total intensity and linear polarization.

In most of current experiments the beam ellipticity is small (we shall refer to these as ''slightly elliptical beams'' in what follows), i.e., the beam full widths along the major and minor axes differ by 10–20 % at most. This implies that, in practice, the perturbative expansion truncated to low orders describes the harmonic transform with high accuracy up to very high multipoles.

The perturbative expansion allows a simple qualitative discussion of the role that different m modes play in the beam transform (see, e.g., Sec. III). In particular, the relative weight of these modes is assessed by working out how they depend on experimental parameters (e.g., width and ellipticity of the beam). This information cannot be directly extracted from a non-perturbative solution.

The full-sky polarization correlation matrix can be most simply discussed for the ''slighly elliptical beams'' for which deviations from the circular Gaussian beam results can be explicitly derived.

In particular, we have obtained analytic solutions for both the total intensity (temperature anisotropy) and linear polarization window functions. The main results are given in Sec. II, Eq. (9) and Sec. V, Eq. (23).

Our findings show that the circular ($m=0$) mode dominates the total intensity window function, although the first non-circular (higher m) modes cannot be neglected in a consistent analysis. The reason for the latter is that higher m modes in the beam transform can be identified amongst the higher-order corrections in the ellipticity expansion around the circular Gaussian window. This provides a simple explanation for previous semi-analytic and numerical results in the literature.

For linear polarization, we found that $m=2$ is the dominant mode but again, higher modes ($m=2,4,\ldots$) must be included to compute accurately the window function.

Numerical integration validates our approach and provides practical prescriptions for how many terms in the perturbative expansion of the circular mode of the window have to be taken to achieve a given accuracy. This in turn translates directly into how many non-circular (higher-m) modes contribute non-negligibly to the window function of the elliptical beam (see Sec. IV A).

We have implemented our analytic solutions for the elliptical window function to derive expressions for the full-sky polarization correlation functions for elliptical beams (see Sec. VI). In particular, we have derived simple analytic expressions for slightly elliptical beams, taking into account the beam orientation and scanning strategy of a given experiment. We find that, for simple scanning strategies, the ellipticity of the beam induces additional correlations of the order of 20% for small angular separations (few beam widths) with respect to a circularly symmetric Gaussian beam.

Finally, we have investigated the impact of beam asymmetry in error estimation for CMB power spectra in the presence of uncorrelated noise. We find that error bars for a circular Gaussian window largely underestimate those of an elliptical window when the pixel noise becomes dominant. However, a good approximation to the actual error bars is given by an *effective circular Gaussian* window of beam width $\sigma_{eff}=\sqrt{\sigma_a\sigma}$, where σ_a and σ are the major and minor axes of the ellipse. Note that for slightly elliptical beams ($\chi\rightarrow 0$), $\sigma_{eff}\approx\sigma(1+\chi/4)$ which is approximately the width of the circular mode of the elliptical window, b_{l0}, as discussed in Sec. II. This explains why for quasi-circular windows, $\sigma_{eff}=\sqrt{\sigma_a\sigma}$ provides an accurate estimate of the power spectra error bars.

We shall emphasize that in our approach we introduce the experimental beam in the *time stream*, while the ''effective beam'' in the *pixel domain* is the result of multiple observations of the same sky pixel with different orientations of the beam (and possibly with a different noise level) for general scanning strategies. This implies that non-circular modes of the effective beam are expected to cancel out to some extent and therefore the ''effective'' circular component of the beam should yield an almost unbiased estimate of the C_l, as shown by recent numerical analysis (see [33]). Therefore the nominal ellipticity in the time domain will be typically larger than the final effective ellipticity on the map. In the discussion of the estimated errors in the power-spectrum presented in Sec. VII, we take the effective ellipticity to be the same as the one defined in the time stream and thus our estimates must be taken only as upper limits to the actual effect of window ellipticity.

The issue of beam asymmetry here discussed is particularly relevant for future high-resolution and sensitivity CMB anisotropy experiments, especially those measuring also polarization, such as the Planck satellite.

In a future work [35], we shall validate the elliptical model for the beam asymmetry presented here in the presence of other systematic effects (non-elliptic beam distortion/asymmetry, pointing errors, other sources of noise, etc.). Such an analysis will show under which circumstances beam ellipticity is a major systematic effect in a realistic analysis of a CMB experiment. Some recent work along these lines has already been done for the Planck satellite [36], although the formalism used is only valid for small patches of the sky.

ACKNOWLEDGMENTS

We would like to thank E. Elizalde, E. Hivon, R. Juszkiewicz, S. Prunet, E. Simonneau, and especially R. Stompor and R. Teyssier for many useful comments and discussions. PF acknowledges the CMBNET for financial support.

APPENDIX A: PERTURBATIVE EXPANSION OF THE ELLIPTICAL BEAM HARMONIC TRANSFORM

In this appendix we present the key steps for the derivation of the spherical harmonic transform for the total intensity beam Eq. (9). In the flat-sky limit ($\theta\rightarrow 0$) the elliptical beam shape can be expressed in Cartesian (x,y),

$$B(x,y)=B_0(\sigma_a,\sigma_b)\exp\left[-\frac{x^2}{2\sigma_a^2}-\frac{y^2}{2\sigma_b^2}\right] \qquad \text{(A1)}$$

where we define σ_a and σ_b as the beam widths in the major x and minor y axes, and the normalization is given by $B_0(\sigma_a,\sigma_b)=1/(2\pi\sigma_a\sigma_b)$.

For analysis on the sphere, it is more convenient to introduce (planar) polar coordinates to describe the beam, $x=\theta\cos\phi$ and $y=\theta\sin\phi$,

$$B(\theta,\phi)=B_0\exp\left[-\frac{\theta^2}{2\sigma_b^2}f(\phi)\right] \tag{A2}$$

where $f(\phi)\equiv 1-\chi\cos^2\phi$ describes deviations from the circular (or axisymmetric) Gaussian window and the ellipticity parameter $\chi\equiv 1-(\sigma_b/\sigma_a)^2$ is defined within the range $1\geqslant\chi\geqslant 0$. The circular Gaussian window is thus recovered for the limiting case $\chi=0$. For the sake of simplicity, we have taken the beam to be pointing to the north pole of the sphere ($\theta=0$).

The spherical harmonic transform of the total intensity beam is defined as

$$b_{lm}=\int d\Omega B(\theta,\phi)Y^*_{lm}(\theta,\phi) \tag{A3}$$

where $d\Omega=d\theta\sin\theta d\phi$ and spherical harmonics are defined as

$$Y_{lm}(\theta,\phi)=N_{lm}P_l^m(\cos\theta)e^{im\phi} \tag{A4}$$

$$N_{lm}=\sqrt{\frac{2l+1}{4\pi}}\sqrt{\frac{(l-m)!}{(l+m)!}} \tag{A5}$$

where P_l^m are the Legendre polynomials and the spherical harmonics obey the conjugation property $Y^*_{lm}=(-1)^mY_{l-m}$. Replacing Eq. (A4) in Eq. (A3) we get

$$b_{lm}=(-1)^mN_{l-m}\int_0^\pi d\theta\sin\theta P_l^{-m}(\cos\theta)\times\int_0^{2\pi}d\phi B(\theta,\phi)e^{im\phi} \tag{A6}$$

In the flat-sky limit ($\theta\ll 1$ rad, $l\gg 1$),

$$P_l^{-m}(\cos\theta)\approx l^{-m}J_m(l\theta) \tag{A7}$$

where J_m is the mth order Bessel function of the first kind. In this limit, the above integral Eq. (A6) reads

$$b_{lm}=(-1)^mN_{l-m}l^{-m}\int_0^\pi d\theta\theta J_m(l\theta)\int_0^{2\pi}d\phi B(\theta,\phi)e^{im\phi} \tag{A8}$$

In order to solve this integral analytically, we introduce a convenient perturbative expansion of the beam in real space in powers of the ellipticity parameter χ,

$$B(\theta,\phi)=B_0B(\theta)\exp\left[\chi\frac{\theta^2}{2\sigma^2}\cos^2\phi\right]=B_0B(\theta)\sum_{n=0}^{\infty}\left(\frac{\theta^2}{2\sigma^2}\right)^n\cos^{2n}\phi\frac{\chi^n}{n!} \tag{A9}$$

where $B(\theta)=\exp[-\theta^2/2\sigma^2]$, which yields an analogous series in harmonic space,

$$b_{lm}=\sum_n b_{lm}^{(n)}\frac{\chi^n}{n!}=b_{lm}^{(0)}+b_{lm}^{(1)}\chi+\mathcal{O}(\chi^2) \tag{A10}$$

The perturbative expansion Eq. (A9) allows us to factorize the 2D integrals of the beam harmonic transform Eq. (A6) in two 1D integrals for θ and ϕ, respectively. Thus the nth order term of the beam transform can be expressed as follows:

$$b_{lm}^{(n)}=(-1)^mN_{l-m}I_{lm}^{(n)}K_m^{(n)} \tag{A11}$$

with

$$I_{lm}^{(n)}=l^{-m}(2\sigma^2)^{-n}\int_0^\pi d\theta\theta^{2n+1}J_m(l\theta)B(\theta) \tag{A12}$$

$$K_m^{(n)}=\int_0^{2\pi}d\phi\cos^{2n}\phi e^{-i2m\phi}. \tag{A13}$$

Making use of Eq. (6.631.1) of [37] and Eqs. (13.1.27), (13.6.9) of [38] one gets

$$I_{lm}^{(n)}=\sigma^{2+m}\frac{(n-m/2)!}{2^{m/2}}e^{-z}L_{n-m/2}^{(m)}(z) \tag{A14}$$

with $z=l^2\sigma^2/2$ and

$$K_m^{(n)}=\frac{2\pi}{2^{2n}}\frac{2n!}{(n+m/2)!(n-m/2)!} \tag{A15}$$

for m even, and $K_m^{(n)}=0$ for m odd. The fact that odd m modes do not contribute to the harmonic transform is due to the parity symmetries of the ellipse. Thus the nth order term of the expansion Eq. (A11) is given by

$$b_{lm}^{(n)}=\frac{2\pi}{2^{2n+m/2}}N_{l-m}\frac{2n!}{(n+m/2)!}\sigma^{2+m}e^{-z}L_{n-m/2}^{(m)}(z) \tag{A16}$$

which replaced in Eq. (A17) yields the final expression

$$b_{lm}=\sigma^mN_{lm}^Ie^{-z}\sum_{\nu=0}^{\infty}\gamma_{\nu,m}L_\nu^{(m)}(z)\chi^{\nu+m/2} \tag{A17}$$

where we define $N_{lm}^I=N_{l-m}/\bar{B}_0$, $\bar{B}_0=B_0/(2\pi\sigma^2)$, and $\gamma_{\nu,m}=(2\nu+m)!/[2^{2\nu+3m/2}(\nu+m/2)!(\nu+m)!]$. The first Laguerre polynomials are

$$L_0^{(m)}(z)=1,\quad L_1^{(m)}(z)=m+1-z$$

$$L_2^{(m)}(z)=\frac{1}{2}[(m+1)(m+2)+z(-4-2m+z)]$$

$$L_3^{(m)}(z) = L_3^{(m)}(z) = \frac{1}{6}\{(m+1)(m+2)(m+3) + z[-3(m+2)(m+3) + z(9+3m-z)]\} \tag{A18}$$

and higher orders can be obtained from the recurrence relation [see Eq. (4.18.1) in [39]]

$$L_n^{(m)}(z) = \frac{1}{n}[(2n-1-x+m)L_{n-1}^{(m)}(z) - (n-1+m)L_{n-2}^{(m)}(z)] \tag{A19}$$

In most practical situations the beam ellipticity is rather small, $\chi \ll 1$. In these cases, one only needs to compute the first terms (two or three terms account for the beam transform up to very large multipoles with high accuracy, see Sec. IV C, Table I).

For example, the beam harmonic transform up to *second order* in the ellipticity expansion has non-vanishing contributions only from the modes $m=0$, 2 and 4, which read

$$b_{l0} = N_{l0} e^{-l^2\sigma^2/2}\left[1 - \frac{\chi}{4} l^2\sigma^2 + \frac{\chi^2}{4}\left(-l^2\sigma^2 + \frac{3}{16} l^4\sigma^4\right)\right]$$

$$b_{l2} = N_{l0} \frac{\chi}{8} l^2\sigma^2 e^{-l^2\sigma^2/2}\left[1 + \chi\left(1 - \frac{1}{4} l^2\sigma^2\right)\right]$$

$$b_{l4} = N_{l0} \frac{\chi^2}{128} l^4\sigma^4 e^{-l^2\sigma^2/2} \tag{A20}$$

where $N_{l0} = \sqrt{2l+1/4\pi}$, and negative modes (i.e., $m=-2,-4$) have to be included as they have the same harmonic transform as positive modes, i.e., $b_{l-m} = b_{lm}$. Similar expressions for the harmonic transform to *first order* in the ellipticty are given in Sec. III, Eqs. (12) and (13). Note that for a circular Gaussian window, $\chi = 0$, one gets, as expected, $b_{l0} = N_{l0} \exp[-l^2\sigma^2/2]$ and $b_{lm} = 0$ for $m \neq 0$.

APPENDIX B: PERTURBATIVE EXPANSION OF THE LINEARLY POLARIZED ELLIPTICAL BEAM HARMONIC TRANSFORM

The aim of this appendix is to provide a detailed derivation of the harmonic transform for linearly polarized elliptical beams, Eq. (23). The spherical harmonic transform of a linearly polarized beam can be written in terms of the Stokes parameters $\tilde{Q}$ and $\tilde{U}$,

$$b_{lm}^G = \frac{1}{2\sqrt{2}} \int d\Omega [(\tilde{Q} - i\tilde{U})_2 Y_{lm}^* + (\tilde{Q} + i\tilde{U})_{-2} Y_{lm}^*] b_{lm}^C$$

$$= \frac{-i}{2\sqrt{2}} \int d\Omega [(\tilde{Q} - i\tilde{U})_2 Y_{lm}^* - (\tilde{Q} + i\tilde{U})_{-2} Y_{lm}^*] \tag{B1}$$

where we define the spin-2 spherical harmonics as[6]

$${}_{\pm 2}Y_{lm} = M_{l,m\ \pm 2}P_l^m(\cos\theta) e^{im\phi} \tag{B2}$$

where

$$M_{lm} = 2\sqrt{\frac{(l-2)!}{(l+2)!}} N_{lm} \tag{B3}$$

and we define a generalization of the Legendre polynomials for spin-2 harmonics,[7]

$${}_{\pm 2}P_l^m(\cos\theta) = -\left(\frac{l-m^2}{\sin^2\theta} + \frac{1}{2} l(l-1)\right) P_l^m(\cos\theta) + (l+m)\frac{\cos\theta}{\sin^2\theta} P_{l-1}^m(\cos\theta) \mp \frac{m}{\sin^2\theta}[(l-1)\cos\theta P_l^m(\cos\theta) - (l+m) P_{l-1}^m(\cos\theta)] \tag{B4}$$

The above quantities obey the following parity conditions:

$${}_{\pm 2}P_l^{-m} = (-1)^m \frac{(l-m)!}{(l+m)!} {}_{\pm 2}P_l^m \tag{B5}$$

$$M_{l-m} = \frac{(l+m)!}{(l-m)!} M_{lm} \tag{B6}$$

which imply that

$${}_{\pm 2}Y_m^* = {}_{\mp 2}Y_{lm} e^{-2im\phi} \tag{B7}$$

which allows us to recast Eq. (B1) in a more convenient way,

$$b_{lm}^G = \frac{1}{2\sqrt{2}} \int d\Omega [(\tilde{Q} - i\tilde{U})_2 Y_{lm} + (\tilde{Q} + i\tilde{U})_{-2} Y_{lm}] e^{-2im\phi}$$

$$b_{lm}^C = \frac{-i}{2\sqrt{2}} \int d\Omega [(\tilde{Q} - i\tilde{U})_2 Y_{lm} - (\tilde{Q} + i\tilde{U})_{-2} Y_{lm}] e^{-2im\phi}. \tag{B8}$$

For a pure co-polar beam (i.e., for an ideal optical system and telescope see [18]), we have

$$\tilde{Q} \pm i\tilde{U} = -B(\theta,\phi) e^{\pm 2i\phi} \tag{B9}$$

where $B(\theta,\phi)$ is defined in Eq. (A2). We have assumed that the beam response is measured in the co- and cross-polar basis defined on the sphere, σ_{co} and σ_{cross}, according to Ludwig's third definition [40],

$$\sigma_{co} = \sin\phi\sigma_\theta + \cos\phi\sigma_\phi$$

[6]Note that ${}_{\pm 2}Y_{lm} = W_{lm} \pm iX_{lm}$, according to the notation used by [17].

[7]The ${}_{\pm 2}P_l^m$ polynomials are simply related to the G_{lm} in [14,17,21]: ${}_{\pm 2}P_l^m(x) = G_{lm}^+(x) \mp G_{lm}^-(x)$.

$$\sigma_{cross} = \cos\phi\,\sigma_\theta - \sin\phi\,\sigma_\phi \tag{B10}$$

where σ_θ and σ_ϕ are the usual spherical polar bases. Such a co- and cross-polarization basis, Eq. (B10), is obtained by parallel transporting the local Cartesian basis defined at the north pole, σ_x and σ_y, along great circles through the poles of the sphere (see, e.g., [18] for a discussion).

Replacing Eq. (B9) into Eq. (B8), one sees that the first term in Eq. (B8) is non-vanishing only for negative m modes while the second term is non-zero for positive m modes alone. What is more, the parity properties of the G and C modes,

$$b^C_{lm} = i b^G_{lm}, \quad b^C_{l-m} = -i b^G_{l-m},$$
$$b^P_{l-m} = b^P_{lm} \quad P = G, C \tag{B11}$$

imply that the harmonic transform of linear polarization can be fully determined from one of the two components alone, say G. Moreover, both negative and positive modes have the same harmonic transform. Thus we shall assume $m>0$ below with no loss of generality. In this case the harmonic transform of the G mode is simply given by

$$b^G_{lm} = \frac{M_{lm}}{2\sqrt{2}} \int d\Omega B(\theta,\phi)\, {}_{-2}P^m_l(\cos\theta) e^{-i(m-2)\phi} \tag{B12}$$

In the flat-sky limit ($\theta \ll 1$ rad, $l \gg 1$),[8]

$${}_{-2}P^m_l(\cos\theta) \approx \frac{1}{2}(-1)^m l^{m+2} J_{m-2}(l\theta) \tag{B13}$$

and thus,

$$b^G_{lm} = (-1)^m \frac{l^{m+2} M_{lm}}{4\sqrt{2}} \int d\Omega B(\theta,\phi) J_{m-2}(l\theta) e^{-i(m-2)\phi} \tag{B14}$$

Introducing the ellipticity expansion, Eq. (A2), one can solve the integral to any perturbative order,

$$b^{G(n)}_{lm} = \frac{1}{2\sqrt{2}} M_{lm} \overline{I}^{(n)}_{lm} \overline{K}^{(n)}_m \tag{B15}$$

with

$$\overline{I}^{(n)}_{lm} = \frac{l^{m+2}}{2} (2\sigma^2)^{-n} \int_0^\pi d\theta\, \theta^{2n+1} J_{m-2}(l\theta) B(\theta) \tag{B16}$$

$$\overline{K}^{(n)}_m = \int_0^{2\pi} d\phi \cos^{2n}\phi e^{-i(m-2)\phi}. \tag{B17}$$

[8]This corrects the expression for the small-angle limit in [14]: the pre-factor l^{m+2} in Eq. (B13) corrects the pre-factor l^{6-m} in Eq. (4.32) of [14].

Noting that the above integrals are basically the same as those for the total intensity beam, Eqs. (A12) and (A13), but replacing m by $m-2$ everywhere, they can be integrated in the same way,

$$\overline{I}^{(n)}_{lm} = \sigma^m \frac{(n-m/2+1)!}{2^{m/2}} e^{-z} L^{(m-2)}_{n-m/2+1}(z) \tag{B18}$$

with $z = l^2\sigma^2/2$ and

$$\overline{K}^{(n)}_m = \frac{2\pi}{2^{2n}} \frac{2n!}{(n+m/2-1)!(n-m/2+1)!} \tag{B19}$$

for even modes $m \geqslant 2$, and $\overline{K}^{(n)}_m = 0$ for m odd. Therefore the nth order term Eq. (B15) in the beam expansion is given by

$$b^{G(n)}_{lm} = \frac{2\pi}{2^{2n+m/2}} M_{lm} \frac{2n!}{(n+m/2-1)!} \sigma^m e^{-z} L^{(m-2)}_{n-m/2+1}(z) \tag{B20}$$

which, introduced in Eq. (B15), finally gives

$$b^G_{lm} = \sigma^{m-2} N^G_{lm} e^{-z} \sum_{\nu=0}^{\infty} \gamma_{\nu,m-2} L^{(m-2)}_\nu(z) \chi^{\nu+m/2-1} \tag{B21}$$

where we define $N^G_{lm} = -l^{2m} M_{lm}/(4\sqrt{2}\overline{B}_0)$, and the coefficients $\gamma_{\nu,m-2}$ are the same as those defined for the total intensity Eq. (A17), except for the subindex which is $m-2$ here instead of m there.

For most of the actual experimental beams the ellipticity is rather small, $\chi \ll 1$. As discussed in Appendix A, a *second order* analysis of the beam ellipticity is already very accurate to very large multipoles as compared with numerical integration shows (see Sec. IV C, Table I for specific prescriptions depending on experimental parameters). Thus, expanding the beam harmonic transform to *second order* in χ one gets non-vanishing contributions only from the modes $m=2$, 4, and 6,

$$b^G_{l2} = -\frac{N_{l0}}{2\sqrt{2}} e^{-l^2\sigma^2/2} \left[1 - \frac{\chi}{4} l^2\sigma^2 + \frac{\chi^2}{4} \left(-l^2\sigma^2 + \frac{3}{16} l^4\sigma^4 \right) \right]$$

$$b^G_{l4} = -\frac{N_{l0}}{2\sqrt{2}} \frac{\chi}{8} l^2\sigma^2 e^{-l^2\sigma^2/2} \left[1 + \chi \left(1 - \frac{1}{4} l^2\sigma^2 \right) \right]$$

$$b^G_{l6} = -\frac{N_{l0}}{2\sqrt{2}} \frac{\chi^2}{128} l^4\sigma^4 e^{-l^2\sigma^2/2} \tag{B22}$$

where $N_{l0} = \sqrt{2l+1/4\pi}$, and negative modes (i.e., $m=-2$, -4, -6) have to be included as they have the same harmonic transform as positive modes, i.e., $b^G_{l-m} = b^G_{lm}$. Analogous expressions for the harmonic transform to *first order* in the ellipticty are given in Sec. V, Eqs. (25) and (26). Note that for a circular Gaussian window, $\chi = 0$, one gets $b^G_{l\pm 2}$

$=-(N_{l0}/2\sqrt{2})\exp[-l^2\sigma^2/2]$ and $b^G_{lm}=0$ for $|m|>2$. Note that, as argued above [see the paragraph under Eq. (B17)], the linearly polarized beam transform, Eq. (B22), can be straightforwardly obtained from the total intensity beam transform, Eq. (A20), by replacing in the latter m by $m-2$, and including a multiplicative normalizing factor of $-1/(2\sqrt{2})$ appropriate for linear polarization modes, see Eq. (B1).

[1] C. Burigana, D. Maino, N. Mandolesi, E. Pierpaoli, M. Bersanelli, L. Danese, and M. R. Attolini, Astron. Astrophys. **130**, 551 (1998).
[2] N. Mandolesi *et al.*, Astron. Astrophys. **145**, 323 (2000).
[3] J.-H.P. Wu *et al.*, Astrophys. J., Suppl. Ser. **132**, 1 (2001).
[4] T. Souradeep and B. Ratra, Astrophys. J. **560**, 28 (2001).
[5] Boomerang experiment web page: http://www.physics.ucsb.edu/~boomerang
[6] MAXIMA-1 experiment web-page: http://cfpa.berkeley.edu/group/cmb/index.html
[7] Planck satellite web page: http://astro.estec.esa.nl/Planck
[8] W. H. Press, S. A. Teukolsky, W. T. Vetterling, and B. P. Flannery, *Numerical Recipes* (Cambridge University Press, Cambridge, England, 1992).
[9] M. J. Rees, Astrophys. J., Lett. Ed. **153**, L1 (1968).
[10] M. M. Basko and A. G. Polnarev, Sov. Astron. **24**, 268 (1980).
[11] N. Kaiser, Mon. Not. R. Astron. Soc. **202**, 1169 (1983).
[12] J. R. Bond and G. Efstathiou, Astrophys. J., Lett. Ed. **285**, L45 (1984).
[13] *Microwave Foregrounds*, edited by A. de Oliveira-Costa and M. Tegmark, ASP Vol. 181 (ASP, San Francisco, CA, 1999).
[14] A. Stebbins, astro-ph/9609149.
[15] U. Seljak, Astrophys. J. **482**, 6 (1997).
[16] M. Kamionkowski, A. Kosowsky, and A. Stebbins, Phys. Rev. Lett. **78**, 2058 (1997).
[17] M. Kamionkowski, A. Kosowsky, and A. Stebbins, Phys. Rev. D **55**, 7368 (1997).
[18] A. Challinor, P. Fosalba, D. Mortlock, M. Ashdown, B. Wandelt, and K. Górski, Phys. Rev. D **62**, 123002 (2000).
[19] M. Zaldarriaga, Phys. Rev. D **64**, 103001 (2001).
[20] K. Ng and G. Liu, Int. J. Mod. Phys. D **8**, 61 (1999).
[21] M. Zaldarriaga, Astrophys. J. **503**, 1 (1998).
[22] B. Wandelt and K. Górski, Phys. Rev. D **63**, 123002 (2001).
[23] D. A. Varshalovich, A. N. Moskalev, and V. K. Khersonskii, *Quantum Theory of Angular Momentum* (World Scientific, Singapore, 1988).
[24] D. M. Brink and G. R. Satchler, *Angular Momentum* (Oxford Univ. Press, Oxford, 1962).
[25] J. N. Goldberg *et al.*, J. Math. Phys. **8**, 2155 (1967).
[26] L. Knox, Phys. Rev. D **52**, 4307 (1995).
[27] M. Zaldarriaga and U. Seljak, Phys. Rev. D **55**, 1830 (1997).
[28] E. Hivon *et al.*, astro-ph/0105302.
[29] S. Hanany *et al.*, Astrophys. J. Lett. **545**, L5 (2000).
[30] A. T. Lee *et al.*, astro-ph/0104459.
[31] C. B. Netterfield *et al.*, astro-ph/0104460.
[32] S. Prunet (private communication).
[33] A. Benoit *et al.*, astro-ph/0106152, web site: http://www.archeops.org
[34] J. Tauber, "The Extragalactic Infrared Background and its Cosmological Implications," International Astronomical Union Symposium No. 204, Manchester, England, 2000.
[35] P. Fosalba *et al.* (unpublished).
[36] L.-Y. Chiang *et al.*, astro-ph/0110139.
[37] I. S. Gradshteyn and I. M. Ryzhik, *Table of Integrals, Series, and Products* (Academic Press, New York, 1965).
[38] *Handbook of Mathematical Functions*, edited by M. Abramowitz and I. A. Stegun (National Bureau of Standards, Washington, DC, 1964).
[39] N. N. Lebedev, *Special Functions & Their Applications* (Dover Publications Inc., New York, 1972).
[40] A. C. Ludwig, IEEE Trans. Antennas Propag. **AP-21**, 116 (1973).